SAR AMBIGUITY STUDY FOR THE CASSINI RADAR

Scott Hensley, Eastwood Im and William T.K. Johnson

Radar Science and Engineering Section
Jet Propulsion Laboratory
California Institute of Technology
Pasadena, CA 91109, USA

ABSTRACT

The Cassini Radar's synthetic aperture radar (SAR) ambiguity analysis is unique with respect to other spaceborne SAR ambiguity analyses owing to the non-orbiting spacecraft trajectory, asymmetric antenna pattern, and burst mode of data collection. By properly varying the pointing, burst mode timing, and radar parameters along the trajectory this study shows that the signal-to-ambiguity ratio of better than 15 dB can be achieved for all images obtained by the Cassini Radar.

1. INTRODUCTION

The Cassini spacecraft, to be launched in 1997 and to arrive at its destination in 2004, will explore Saturn and its many satellites. One of the science instruments aboard the spacecraft is a multi-mode Ku-band radar, which will be used extensively during the Cassini mission for obtaining surface imagery, topography, slid backscattering measurements of Titan, the perpetually cloud-covered moon of Saturn [1]. Among the radar modes is a synthetic aperture radar imaging mode which v., ill obtain surface imagery at resolutions between 300 m and 3000 m. The SAR is a 5-beam radar operating at 13.8 GHz up to altitudes of 4000 km. The five radar antenna beams will be generated by five off-axis feeds in order to increase the spatial coverage [1].

In order to obtain SAR imagery of sufficient quality to ascertain useful information concerning Titan's surface it is important to keep the returns from regions which are ambiguous in both time and frequency from contaminating the desired signal. Ambiguous returns in the time domain (range direction) result from the inherent inability to associate unambiguously the reflected signal with the corresponding transmitted pulse. This time ambiguity translates into a range ambiguity that is an integer multiple of $c/(2\,PRF)$, where c is the pulse propagation speed and PRF is the radar pulse repetition frequency. The ambiguity in the frequency domain (azimuth direction) arises from the discrete sampling of the echoes which is done to extract azimuth information (Nyquist Theorem). Since azimuth sampling is done at the PRF, scatterers which are separated in frequency by multiples of the PRF will be ambiguous with respect to the desired imaging region. The overall corltalnilla[ion can be quantified by computing the signal-to-ambiguity ratio (STAR) which is the ratio of the dc.sired return signal to the sum of the returns from all ambiguous regions on the surface. The current STAR requirement on the Cassini radar images is 15 dB. Similarly, range and azimuth signal-to-ambiguity ratios can be computed where only the range or azimuth ambiguous regions respectively are used. This information can be used to help the selection of the best radar system parameters to maximize the S'I"Al<.

For the Cassini Radar the computation of ambiguities requires a level of attention 10 several parameters usually not necessary for Earth-orbiting SARs. These parameters include the non-orbiting flyby trajectories, asymmetric antenna beamshapes, and burst mode of data collection. In this paper we will present the unique aspects of the Cassini Radar SAR ambiguities. Section 2 covers the Cassini Radar ambiguity factors and a brief discussion on the computation and maximization of the STAR is given in section 3. Some simulation results based on realistic geometric aod radar system parameters will also be presented.

2. CASSINI RADAR AMBIGUITY FACTORS

2.1 **Cassini Radar Antenna** -- The amount of ambiguous energy contained in each synthetic aperture is affected by the antenna pattern, the trajectory, the pointing direction, the radar pulse timing parameters, and the backscatter function of the surface being imaged. Of these factors the most important factor mitigating the amount of ambiguous returned energy is the antenna pattern. If a narrow beam is used to image the desired surface region and all the ambiguous regions fall in the antenna sidelobes then the ambiguous signals are greatly reduced. Due to the limited spacecraft weight and volume, the Cassini radar is forced to utilize the spacecraft's high gain 4 m telecommunications parabolic reflector antenna for signal transmission and reception. In order to achieve the desired surface coverage during the limited number of Titan flybys a multiple feed structure at 13.8 GHz is mounted on the antenna reflector to generate five antenna beams which overlap in the range direction. The center circular beam (beam 3) is generated by illuminating the entire reflector with the feed that is located at the reflector's focal position, while the four side-tookiog beams are generated by partially illuminating the reflector with feeds that are offset from the reflector's focal axis by the appropriate amounts. Due to feed symmetries the Iwo outermost beams (1 and S) and the Iwo inner beams (2 and 4) have identical, patterns except that they are rotated 180° with respect to one another. Beams 1 through S will illuminate swaths that are progressively further from the satellite's nadir track. Expected parameters for the 5 beams are shown in Table I.

Table I. Cassini Radar Beam Parameters

Parameter	Beams 1 & 5	Beams 2 & 4	Beam 3
Peak Gain (dBi)	45.8	46.1	53.1
Azimuth Beamwidth (deg)	0.35	0.35	0.35
Range Beamwidth (deg)	1.35	1.35	0.35
Angle From Focal Axis (deg)	**2,20**	0.85	**00**
Peak Sidelobe (dB)	-120	-13.0	-20.0

Figure I shows the antenna pattern for beams 2 and 4. Note the non-uniform drop-off in gain in the azimuth direction as well as the asymmetric sidelobe structure. This asymmetry causes the ambiguous regions on either side of the desired illumination region 1 0 contribute in an asymmetric fashion to the STAR and hence complicates the selection of the optimal radar operating parameters. likewise beams 1 and 5 have aysmmetric beam shapes due to the offset antenna feeds.

2.2 **Radar Timing** -- During SAR operation, the spacecraft will rotate either 10 the left side or right side of the sub-satellite track and all five of the radar antenna beams will be used sequentially to maximize the cross track coverage. The relatively large uncertainties in the spacecraft ephemeris and attitude predictions at the time of data collection have led to a non-interleaved, "burst timing" design for signal transmission and reception. In this design the radar will transmit a series of pulses (30-100) from one of the five antenna beams and then after a period approximately equal to the 2-way propagation time will switch to receive echoed pulses and the switch to the next beam.

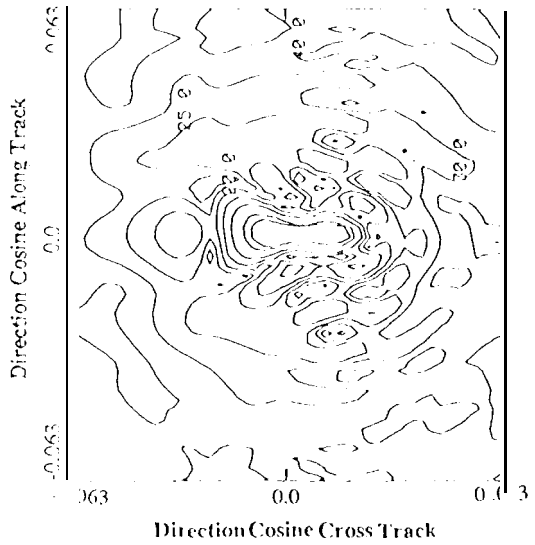

Figure 1. Contour plot of beams 2 and 4 antenna pattern.

For a conventional SAR that continuously transmits and recieves on a per PU lse basis, a scatterer undergoes a continuous change in frequency while being illuminated by the antenna beam. The PRF is generally selected to be greater than the total change in frequency during which the same scatterer is within the 3 dB azimuth beamwidth. Ambiguous returns are generated from all scatterers that are separated by multiples of the PRF in frequency [?]. On the other hand, with "burst timing" operation any particular scatterer on the surface will be illuminated by only those portions of the azimuth beamwidth when the radar is transmitting bursts. Viewed in the frequency domain this corresponds to the doppler frequencies seen by the SAR when the target is illuminated during the bursts. To account for this effect, we have adapted a frequency-domain "masking" approach, similar to that used by the Magellan radar design analysis [3] 10 quantify the SAR imaging performance. The mask adds signal and ambiguity energies contributed by targets during the times they are actually illuminated. The simplicity of the mask approach arises from the fact that the masking function depends only on the interburst period and the burst on time. The number of spikes in the mask across the doppler spectrum corresponds to the number of locks that are obtained. The spacing between the spikes is determined by the interburst period and the width of each is spike determined by the burst duration.

2.3 **Cassini Trajectory** -- The Cassini spacecraft trajectory during Titan SAR imaging encounters is well approximated as a hyperbolic trajectory having periapsis altitudes varying from 950 km to 1500 km. The SAR will sequentially collect burst data on each of the five beams up to an altitude of 4000 km. During SAR data acquisition the imaging geometry will undergo a large variation in pitch angle (between -60" and + 60°). The pitch angle is the angle the velocity makes with the local horizontal. This variation, when coupled with the small wavelength, results in large isodoppler curvatures. "1 he curvature, which varies throughout the entire pass and between different passes, must be compensated for either during ground processing or by continuous spacecraft attitude adjustment, in order to align the sylllll]c.sized apertures properly with the illuminated radar footprint areas, Figure 2 shows an example of the ambiguity geometry and the antenna footprint geometry for the Cassini radar beam 1 when the pitch angle is equal [o -56,"/", Note that the data collection window crosses beyond the 3 dB footprint of the antenna in the far range due 10 the extreme isodoppler curvature.

By squinting the beam appropriately the change in doppler with respect to range, $\partial f/\partial r$, can be forced 10 zero at the center of the swath. Note that this is not the same as steering 10 zero doppler as is done with Earth orbiting SARs, although the plane of zero doppler also has $\partial f/\partial r = 0$. The zero doppler plane dots not in general intersect the planet for a hyperbolic trajectory. Figure 3 shows the same radar configuration with the radar squinted + 16.5° with respect to broadside. Note that the data collection window now remains within the antenna footprint. Alternatively, it is possible to correct for $\partial f/\partial r$ in the processor and keep tbe data collection window within the antenna footprint.

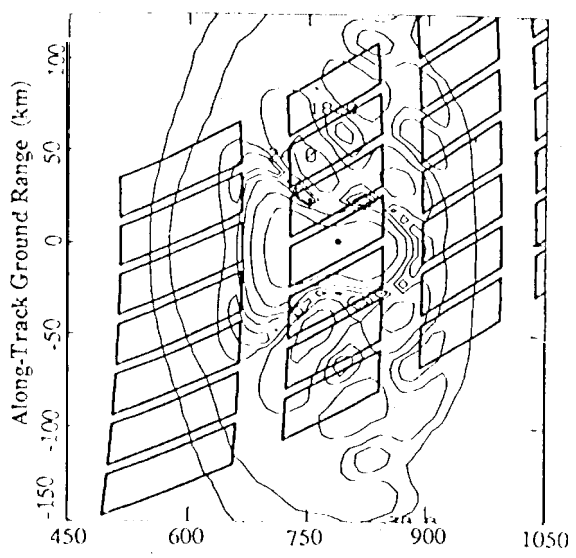

Figure 2. Cassini Radar ambiguity and antenna footprint geometry. The rectangular regions are the desired data collection region and the ambiguous regions. The solid dot is the boresight location in the desired data region.

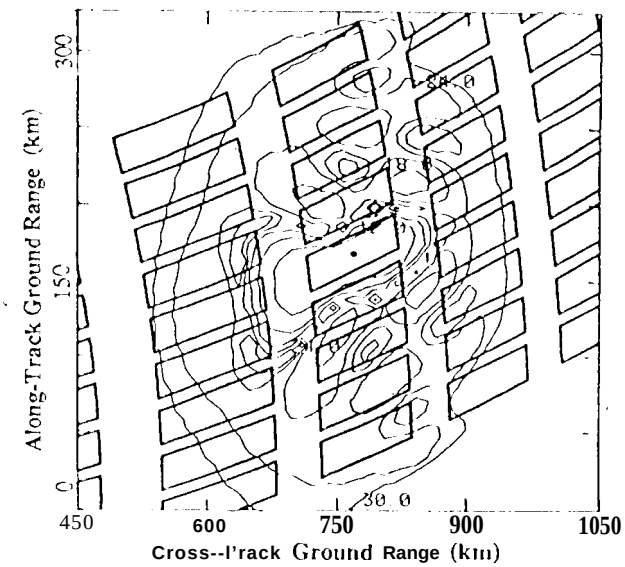

Figure 3. Cassini ambiguity and antenna footprint geometry for a + 16.5°squint.

2,4 **Surface Backscatter** -- Another important factor affecting the STAR is the surface backscattering properties as a function of incidence angle. Little information is currently available concerning Titan's scattering properties. For the purpose of this study we have elected 10 use the Muhleman backscattering function given as

$$\sigma_o(i) = \frac{k_1 \sin(i)}{\sin(i) + k_2 \cos^3(i)} \qquad (1)$$

where i is the incidence angle and k_1 and k_2 are constants that depend on the surface properties.

3. SIMULATION ANI) RESULTS

Simulations were conductedto access the signal-to-ambiguity levels at various points along the Cassini spacecraft trajectory. In the simulation, the PRF, burst period, burst on time, squint angle, processing bandwidth (portion of the azimuth spectrum that is retained after SAR processing), and range gait length (data collection window size in range) were varied to optimize the STAR.

Five points along the trajectory were selected fca analysis, they were at times since periapsis ('TS 1') equal to O, ±360 sec, ±960 sec. The ±360 sec points are points in the trajectory w here the radar range bandwidth changes from 425 KHz to 850 KHz and the ± 960 sec points are the terminal points for SAR data collection. At each of the selected points the STAR was computed for all five antenna beams.

Computation of the STAR requires a formula for the power reflected back toward the radar from an arbitary area element, Σ, on the surface. The reflected power is obtained from the radar equation and can be written as

$$P_\Sigma = k \iint_\Sigma \frac{\chi^2(\zeta)\, G^2(\zeta)\, \sigma_o(\zeta)}{r^4(\zeta)\, l_a(\zeta)}\, d\zeta \qquad (2)$$

where k is a constant which is independent of the area element Σ, G is the 1-way antenna gain, σ_O is the surface backscatter function, r is the slant range, la is the loss due to atmospheric absorption, χ is the waveform ambiguity function which accounts for mismatch losses due to differences in both range and doppler between a particular differential area element and the element which contains the unambiguous return, and dζ is the differential area element of the surface. In section 1 a characterization of the unambiguous region, Σ_O, and the area elements, Σ_{ij}, which are ambiguous to that region in terms of range and doppler frequency was given. It is useful then to rewrite Equation 2 in terms of range and doppler, since these are the coordinates for which the unambiguous and ambiguous regions are most easily parametrized. Using the following transformation

$$d\zeta = \frac{r^2}{\cos i}\, d(\cos\theta)\, d\gamma = \frac{\lambda r^2}{2v \cos i}\, df d\gamma \qquad (3)$$

where θ is the doppler angle (angle between the velocity vector and the look direction), γ is the range angle measured in the plane perpendicular to the velocity vector, i is the incidence angle, λ is the radar wavelength, and v is the velocity yields

$$P_\Sigma = k \frac{\lambda}{2v} \iint_\Sigma \frac{\chi^2\, G^2(f,\gamma)\, \sigma_o(f,\gamma)}{r^2(f,\gamma) \cos(i(f,\gamma))\, l_a(\gamma)}\, df d\gamma \qquad (4),$$

It is important to note that Equation 4 is exact for a spherical body. Since Titan has a relatively small radius of 2575 km and will be imaged at distances close to twice its radius, flat body approximations will be inadequate for ambiguity computations. The STA}< is then given by

$$STAR = \frac{P_{\Sigma_o}}{\sum_i \sum_j P_{\Sigma_{ij}}} \qquad (5)$$

where $P_{\Sigma O}$ is the unambiguous return and $P_{\Sigma ij}$ are the returns from the ambiguous regions. All the parameters in Equation 4 can be computed directly from the geometry of the orbit and the radar parameters with the exception of the antenna gains. For this we used antenna patterns supplied by the manufacturer of the antenna for the Cassini spacecraft.

The optimization procedure was carried out by iteratively changing various system parameters described above and observing the resulting effect on the total STAR as well as on the range and azimuth STARs. By comparing the range and azimuth ambiguity levels and examining contour plots of the STARs of individual pixels in the beam footprint general gradient information for altering the parameters is ascertained. The major parameters effecting the STAR for the Cassini radar are the PRF and the squint angle, although to get STARS above 15 dB it was necessary to adjust the other parameters as well. Figure 4 shows the total, range and azimuth ambiguities for beam 5 at time since periapsis (TSP) equal -960 sec. These results indicate that azimuth ambiguities are dominating the ambiguous returns, which necessitates setting the PRF to as large as possible. in fact, the optimal PRF is substantially larger than the standard 2v/l (l is the antenna diameter) formula would predict. 'Table II summarizes the STARs that were achieved for tact] of the five beams al the study points along the trajectory.

Through this study we have found that the current optimization procedure requires manual observation and interpetation, and therefore is rather time consuming. Research to automate this procedure is currently being pursued.

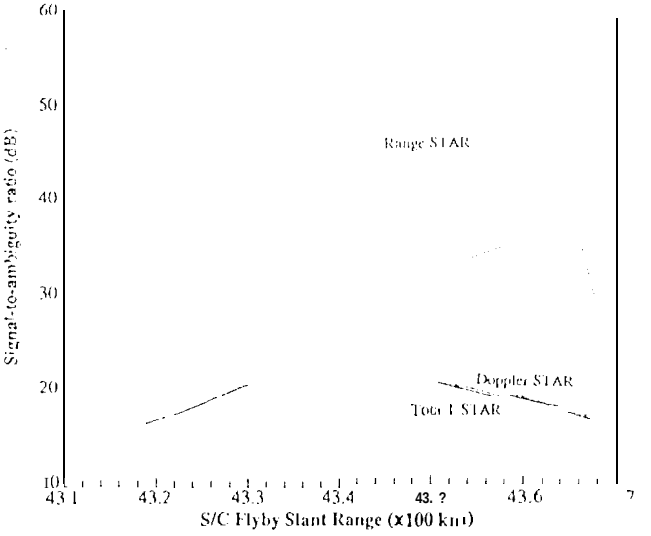

Figure 4, Total, range and azimuth signal-to-ambiguity ratio's as a function of slant range for beam 5 at TSP = -9 60 sec.

Table II. Cassini Radar STAR Performance (dB)

Beam Number	TSP = 960 sec BW = 425KHz	TSP = 360 sec BW = 425KHz	TSP = 360 sec BW = 850KHz	TSP = 0 sec BW = 850KHz
1	15.4	15.1	15.2	15.7
2	15.3	15.3	15.8	15.9
3	25.6	26.1	25.7	23.4
4	16.1	15.9	16.2	16.0
5	15.7	15.3	15.3	15.7

SUMMARY

The Cassini Radar synthetic aperture radar ambiguity analysis is unique with respect to other space borne SAR ambiguity analyses owing to the non-orbiting spacecraft trajectory, asymmetric antenna pattern, and burst mode of data collection. By properly varying the pointing, burst mode timing, and radar parameters along the trajectory this study shows that the signal-to-ambiguity ratio of better than 15 dB can be achieved for all images obtained by the Cassini Radar.

ACKNOWLEDGMENT

The authors would like to thank Alenia Spazio S.p.A. for the antenna patterns provided for this study. The research described in this paper was performed by the Jet Propulsion Laboratory, California Institute of Technology, under contract with the National Aeronautics and Space Administration.

REFERENCES

[1] E. Im and W.T.K Johnson and S. Hensley, "Cassini Radar for Remote Sensing of Titan - Design Considerations", to be presented in IGARSS' 93

[?] Li, F.K. and W.T.K. Johnson, "Ambiguities in Spaceborne Synthetic Aperture Systems", *IEEE Trans. Aerospace and Elec Sys.*, AILS-19(3), pp. 389-395,

[3] W.T.K. Johnson, "Magellan Imaging Radar Mission To Venus", *Proceedings of the IEEE*, Vol. 79, No.6, 1991, pp -/-/'/-790.